Quaternary Research 73 (2010) 107–117

Contents lists available at ScienceDirect

Quaternary Research

journal homepage: www.elsevier.com/locate/yqres

A bimillennial-length tree-ring reconstruction of precipitation for the Tavaputs Plateau, Northeastern Utah

Troy A. Knight [a,b,*], David M. Meko [b], Christopher H. Baisan [b]

[a] Department of Geography and Regional Development, University of Arizona, Tucson, AZ 85721, USA
[b] Laboratory of Tree-Ring Research, University of Arizona, Tucson, AZ 85721, USA

ARTICLE INFO

Article history:
Received 18 December 2008
Available online 3 October 2009

Keywords:
Tree-rings
Dendroclimatology
Drought
Climate
Utah

ABSTRACT

Despite the extensive network of moisture-sensitive tree-ring chronologies in western North America, relatively few are long enough to document climatic variability before and during the Medieval Climate Anomaly (MCA) ca. AD 800-1300. We developed a 2300-yr tree-ring chronology extending to 323 BC utilizing live and remnant Douglas-fir (*Pseudotsuga menziesii*) from the Tavaputs Plateau in northeastern Utah. A resulting regression model accounts for 70% of the variance of precipitation for the AD 1918–2005 calibration period. Extreme wet and dry periods without modern analogues were identified in the reconstruction. The MCA is marked by several prolonged droughts, especially prominent in the mid AD 1100s and late 1200s, and a lack of wet or dry single-year extremes. The frequency of extended droughts is not markedly different, however, than before or after the MCA. A drought in the early AD 500s surpasses in magnitude any other drought during the last 1800 yr. A set of four long high-resolution records suggests this drought decreased in severity toward the south in the western United States. The spatial pattern is consistent with the western dipole of moisture anomaly driven by El Niño and is also similar to the spatial footprint of the AD 1930s "Dust Bowl" drought.

Introduction

One of the most important achievements of North American paleoclimatic research has been the construction and continuing expansion of a continent-wide network of high-resolution climate-sensitive tree-ring chronologies. Despite the improved understanding of late Holocene climate conditions and change afforded by this network, relatively few tree-ring records are available prior to AD 1000, even in the densely sampled semiarid regions of western North America (Cook et al., 2004). Though this region boasts the greatest number of well-replicated millennial-length chronologies, their spatial coverage, species diversity and environmental setting are limited (Stahle et al., 2007). Most millennial-length chronologies are either from high-elevation sites (Hughes and Graumlich, 1996; Hughes and Funkhouser, 1998) or rely on archaeological samples for much of their length (Dean et al., 1985). While both types of chronologies have been useful in illuminating the climatic history of the west, the former is limited by a restricted or mixed environmental response, and the latter by a reduced ability to capture lower frequency (multi-decadal to centennial) climate variability (Cook et al., 1995). Over the past decade, efforts to address these limitations have been made by developing millennial-length, moisture-sensitive chronologies in lower elevation landscapes through utilization of remnant wood (logs, stumps, snags) (e.g., Grissino-Mayer, 1996; Meko et al., 2007).

In this paper we introduce a new tree-ring chronology constructed from living and dead Douglas-fir (*Psuedotsuga menziesii*), and a 2300-yr reconstruction of annual precipitation for the West Tavaputs Plateau of northeastern Utah. Our reconstruction adds 1500 yr to the record of climate history of northeastern Utah, and allows study of modern and past climatic variation from the perspective of the past 2000 yr. A motivation for this work was need for better information on the Medieval Climate Anomaly (MCA) (~AD 800–1300), perhaps the most significant long-term moisture anomaly in the western United States in the past two millennia (Hughes and Diaz, 1994; Cook et al., 2004; Graham et al., 2007). In the American West, numerous proxy records show this period as punctuated by prolonged and severe droughts unlike any in modern times (Stine, 1994; Benson et al., 2002; Cook et al., 2004; Meko et al., 2007). Recent dendroclimatic reconstructions in the Uinta Basin and Uinta Mountains of northeastern Utah highlight unusual wetness in the early 20th century (Carson and Munroe, 2005; Gray et al., 2004; MacDonald and Tingstad, 2007) and agree that some droughts in past centuries were more intense and prolonged than those of the instrumental record. But the longest of these reconstructions extends only to AD 1226, near the end of the MCA. In summarizing the longer record, we focus our analysis on three temporal scales: centennial, decadal, and annual. We identify

* Corresponding author. Fax: +1 520 621 2889.
E-mail address: tak@email.arizona.edu (T.A. Knight).

0033-5894/$ – see front matter
doi:10.1016/j.yqres.2009.08.002

changes in mean conditions and in the frequency and temporal distribution of extremes. We highlight a major drought in the first millennium AD, place droughts of the MCA and the period of modern observations in the context of the past 2000 yr, and examine the relationship between remote atmospheric/oceanic climatic drivers and moisture variability in the Tavaputs region.

Study area

The Tavaputs Plateau lies at about 40°N longitude in northeastern Utah and northwestern Colorado and constitutes the northernmost extent of the Colorado Plateau (Fig. 1). The western sub-plateau, west of the Green River, is the focus of this study. The plateau, whose elevation ranges from 1450 m to 3050 m, is highly dissected and features a labyrinth of steep-walled canyons. Much of the plateau is overlain by sedimentary rocks of the Green River Formation deposited in an Eocene inland lake. Vegetation patterns on the plateau generally depend on elevation and aspect, but are also influenced by cold-air drainage and other factors. Vegetation grades from salt desert scrub (*Atriplex* spp.) at the lowest elevations to mixed conifer and aspen (*Populus tremuloides*) forest at the highest elevations. Piñon (*Pinus edulis*)/juniper (mostly *Juniperus osteosperma*) woodland, sagebrush (*Artemesia spp.*) steppe, and Douglas-fir (*Psuedotsuga menziesii*) forest occupy the middle elevations.

Climate of the plateau and northeastern Utah in general is arid-to-semiarid continental, with precipitation amounts and temperature largely dependent on elevation. The plateau receives precipitation year-round with a high in March, a low in June, and a secondary peak from August through October. Precipitation is most variable in September and October. The primary sources of moisture in the Tavaputs region include frontal systems originating in the Pacific during winter, the North American Monsoon (NAM) in summer, and cutoff lows in late summer and early fall (Mock, 1996). Cutoff lows in September and October may bring excessive and persistent rains to the area and can make the difference between a year being wet or dry. Though this area marks the modern northernmost penetration by the NAM (Mitchell, 1976; Mock, 1996), the northward extent of the NAM has likely shifted through time (Peterson, 1994). Runoff from the plateau contributes to the Green River, a major tributary of the Colorado River.

Data

Tree-ring data

We collected Douglas-fir tree-ring samples from living trees and remnant wood in two side canyons of the plateau's primary drainage, Nine Mile Canyon, at elevations 2130–2225 m. Tree-ring series derived from these two sites are referred to from here on as the Harmon Canyon (HAR) chronology. Cores were taken from living trees by increment borer and cross-sections from remnant wood by chain saw. Both sites have poorly developed soil, sparse ground cover and low density of trees on steep rocky slopes. The conditions are ideal for climate-sensitive ring growth as soil-moisture retention is highly limited and competition among trees and disturbance is minimized (Fritts, 1976). The open-stand conditions and sparse fuels limit fire hazard, allowing extraordinary longevity of trees in addition to the accumulation and preservation of remnant wood. Remnant-wood samples were collected both on slopes where dead trees were found *in situ*, and on the canyon floor where debris-flow deposits emanated from secondary gullies.

Samples were prepared using standard dendrochronological techniques (Stokes and Smiley, 1968). Archaeological reference chronologies for the Four Corners region developed and held at the Laboratory of Tree-Ring Research helped confirm the crossdating of the older portion of the chronology. After measuring rings to the nearest 0.01 mm, we checked crossdating accuracy statistically with the program COFECA (Holmes, 1983).

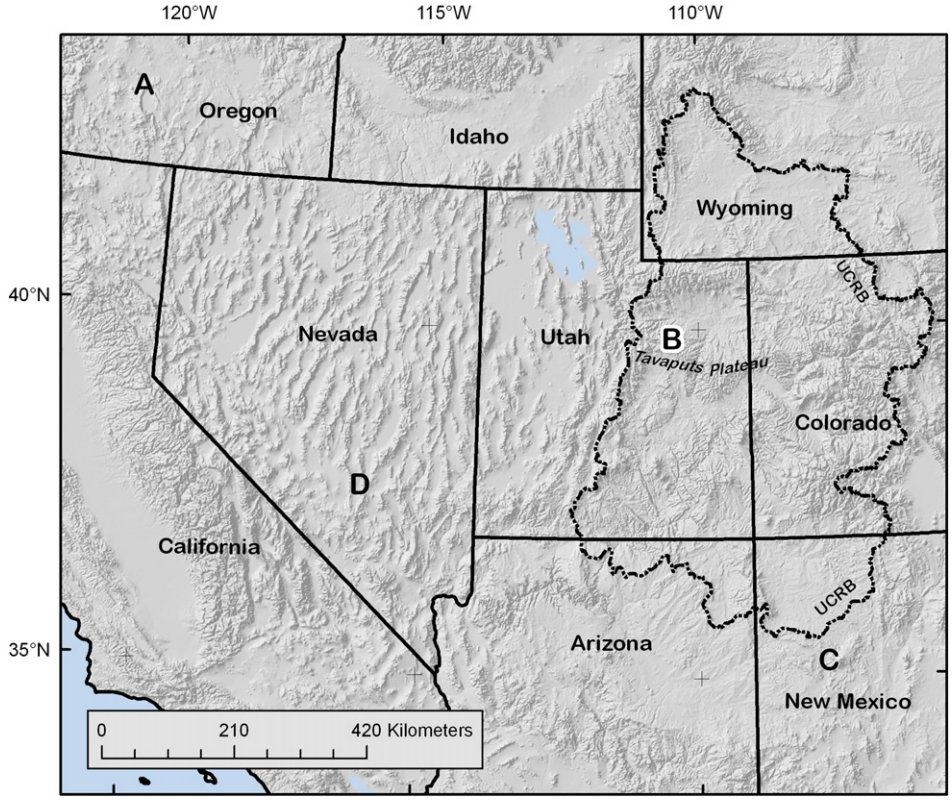

Figure 1. Map of southwestern United States showing site locations. Upper Colorado River basin (UCRB) outlined by dashed line. Letters mark Harmon Canyon tree-ring site on the Tavaputs Plateau (B), and other tree-ring sites and climate reconstructions plotted in Figure 8 (A, C, D). See caption in Figure 8 for details.

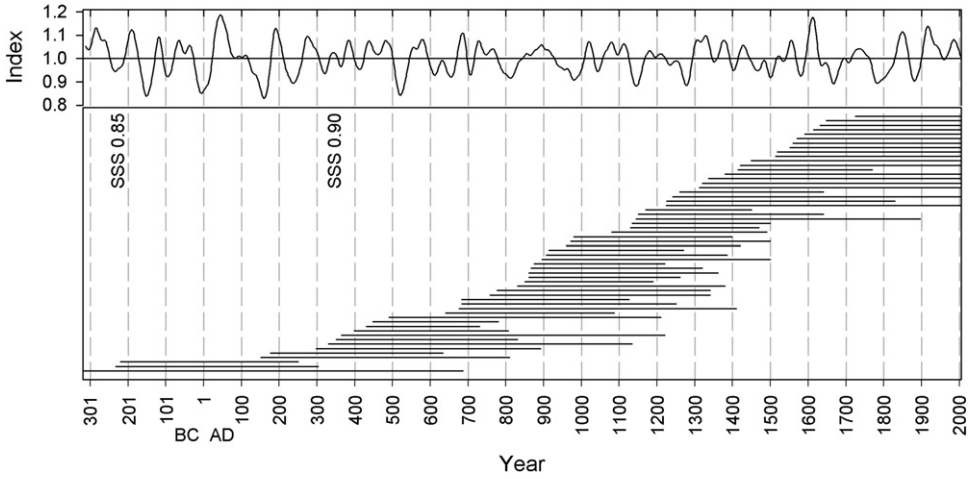

Figure 2. Sample depth of Harmon Canyon tree-ring chronology through time. Top: chronology smoothed with 50-yr spline. Bottom: time coverage by ring-width series for individual trees. These dates do not necessarily reflect establishment and death dates, due to erosion of outer rings, non-presence of pith, etc. Annotated are subsample signal strength (Wigley et al., 1984) thresholds of 0.85 and 0.90.

Measured ring-width series were standardized into a tree-ring chronology using the program ARSTAN (Cook, 1985). We excluded any tree less than 250 yr in age to avoid loss of low-frequency variance associated with detrending of short segments (Cook et al., 1995). Approximately 2/3 of the sampled series were detrended with negative exponential curves or straight lines, and the remainder with a cubic smoothing spline (Cook and Peters, 1981) with a 0.5 frequency response at 70 percent of the series length or 250 yr, whichever was longer. Indices were calculated by the ratio method for each measured radius (Fritts, 1976), and then averaged within trees to produce tree indices. These were then averaged over trees by a biweight mean to generate the site chronology. Variance stabilization options in ARSTAN were explored but not used as they produced inconsequential changes to the chronology. All subsequent analysis uses the "residual" site chronology, which ARSTAN produces by prewhitening (removing autocorrelation from) core indices before averaging over cores or trees.

The high mean between-tree correlation ($r^{-} = 0.86$) of the final HAR chronology indicates that growth variations at the site are driven by a common environmental factor. The mean sensitivity, a measure of high-frequency ring-width variance (Fritts, 1976), is 0.48, which is reasonably high for tree-ring chronologies typically used in climate reconstruction. The chronology includes 58 trees (19 living and 39 dead), and the mean segment-length of the indices for individual trees is 516 yr (Fig. 2). Though the chronology extends to 323 BC, the subsample signal strength does not exceed the suggested minimum threshold of 0.85 (Wigley et al., 1984) until 217 BC, when the sample size reaches two trees.

Climate data

Because the remote Tavaputs Plateau is not well represented by instrumental climate records, we used interpolated climate data to investigate tree growth/climate relationships. Precipitation data came from the Parameter-elevation Regressions on Independent Slopes Model (PRISM) (*http://www.prism.oregonstate.edu/*). PRISM uses weather station data, digital elevation models, and other spatial datasets combined with expert knowledge of climatic processes to derive gridded estimates of monthly precipitation across landscapes (Taylor et al., 1995). PRISM data were downloaded for six grid cells, each with a resolution of 4 km, across the northwestern portion of the plateau and centered on the tree-ring collection sites. The longer axis of the set of cells trends east-west, reflecting the plateau's drop in elevation from east to west. We averaged monthly values from all six points to create a mean Tavaputs precipitation series.

Reconstruction

Correlation analysis was used to identify the season of strongest precipitation signal in the tree-ring chronology. Climate data for this analysis included the PRISM precipitation data summed over 1, 3, 6 and 12 months ending with September of the growth year.

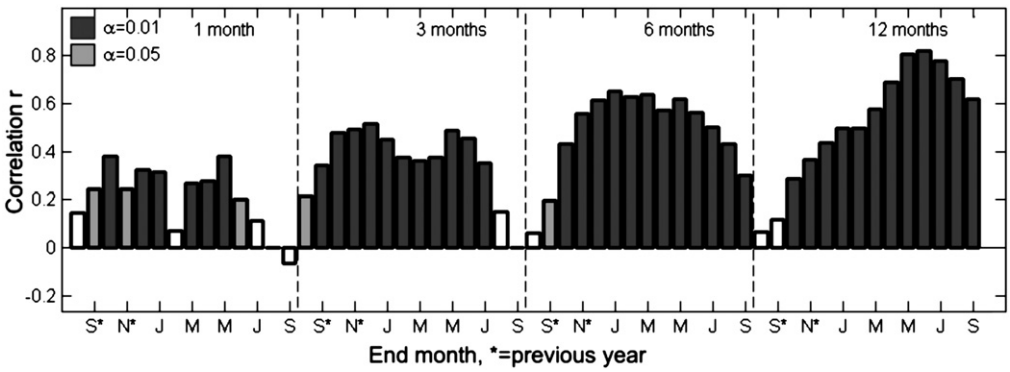

Figure 3. Correlations between the tree-ring chronology and monthly and seasonal PRISM precipitation. Month is end month of the seasonal grouping. Last month is September of growth year. Asterisk indicates months or seasons for year preceding growth year. Significance ($\alpha = 0.01$ and $\alpha = 0.05$) tested by a Monte Carlo method (see text).

Table 1
Calibration and validation statistics of reconstruction model.

Calibration period	Timespan	Calibration		Validation				
		R^2 adjusted	Std error	Sign test hits	Sign test misses	RE	r	RMSE
Late	1962–2005	0.78	42.76	36	8	0.57	0.79	
Early	1918–1961	0.62	47.04	38	6	0.72	0.88	
Full	1918–2005	0.70	46.04					46.6

All validation tests based on split sample method except root-mean-square error (RSME), which is from leave-one-out method.

Significance of correlations was tested by a Monte Carlo approach in which the sample correlations were compared with correlations between precipitation and simulated tree-ring series. The simulated tree-ring series were generated by "exact simulation" following Percival and Constantine (2006). In exact simulation, the spectrum of an observed series is first estimated by one of several possible methods. Circulant imbedding, which uses sampling of Gaussian noise and a frequency-domain approach (Davies and Harte, 1987), is then applied to generate the simulations. In our implementation, we used the periodogram for the spectral estimate (Bloomfield, 2000), and the Deitrich and Newsam (1997) method for circulant embedding. The method was used to generate 1000 simulations of the tree-ring chronology. These were then correlated with the precipitation series, and the 0.95 and 0.99 probability points of the 1000 sample correlations were taken as thresholds for significance.

Correlations reveal a highly significant relationship between the tree-ring chronology and PRISM-derived precipitation. Precipitation in the prior fall and winter appear to be important to Douglas-fir radial growth in the study area (Fig. 3). Correlations of the tree-ring chronology with precipitation increase as months are aggregated into seasons and are highest for the 12-month season grouping of previous July to current June ($r = 0.84$).

The reconstruction model is a regression of annual (July–June) PRISM precipitation on the tree-ring chronology. The model was calibrated on AD 1918–2005. Although PRISM data extends back to AD 1895, station coverage before 1918 was judged too thin to adequately represent climate variations both north and south of the plateau.

The model accounts for more than two-thirds of the variability of precipitation in the calibration period ($R^2_{adj} = 0.70$) (Table 1). Residuals analysis showed no evidence of violation of regression assumptions. Normality of residuals was supported visually by inspection of the histogram and statistically by a Kolmogorov–Smirnov test. Lack of autocorrelation of residuals was supported by the results of a Durbin–Watson statistic and by the plotted autocorrelation function. A scatter plot showed no dependence of residuals on fitted values. The regression was validated by a split-sample method in which the model is fit to one half of the data and tested on the other half (Snee, 1977). Validation included a sign test applied to signs of departures from the mean (Fritts, 1976), the reduction-of-error (RE) statistic, which measures the skill of prediction relative to climatology (the calibration-period mean) (Fritts et al., 1990), and the Pearson correlation between predicted and actual values. The root-mean-square error (RMSE) from cross-validation (Michaelsen, 1987) of the model calibrated on the full AD 1918–2005 period was used as an estimate of uncertainty of the long-term reconstruction.

Validation results show the reconstruction has positive skill (Table 1). The sign test is significant for validation on either half of the data, and RE values are well above 0. Correlation coefficients for the split-sample validation periods are also large and significant. The RMSE of cross-validation of the full model (46.6 mm) is considerably smaller than the standard deviation of the observed precipitation for the AD 1918–2005 full-period calibration (84.2 mm). The reconstruction tracks the observed precipitation closely (Fig. 4). Correspondence is good even for AD 1896–1917, which precedes the period used for computation of calibration and validation statistics and may have somewhat less reliable precipitation data.

Analysis of reconstruction

Methods

We evaluated the Tavaputs precipitation reconstruction, which spans 323 BC to AD 2005, at centennial-to-multidecadal, decadal, and annual scales. We restrict our more detailed analysis of decadal to annual variability of the reconstruction to the period after AD 200, when the chronology consists of 4 or more trees. For multi-decadal to centennial-scale variability we smoothed the reconstruction with 50- and 100-yr splines. At the decadal scale, we quantified duration and severity of wet and dry periods by smoothing the reconstruction with a 19-weight Gaussian filter whose wavelength of 50% frequency response is approximately the same as for an 11-yr moving average (Meko and Woodhouse, 2005). A wet or dry decadal episode was defined as an unbroken interval with the Gaussian-smoothed series above or below its long-term mean.

Within decadal episodes we identified periods of extreme wet or dry conditions as Z-scores of the Gaussian smoothed series exceeding an absolute value of 1.25. This threshold was reached four times

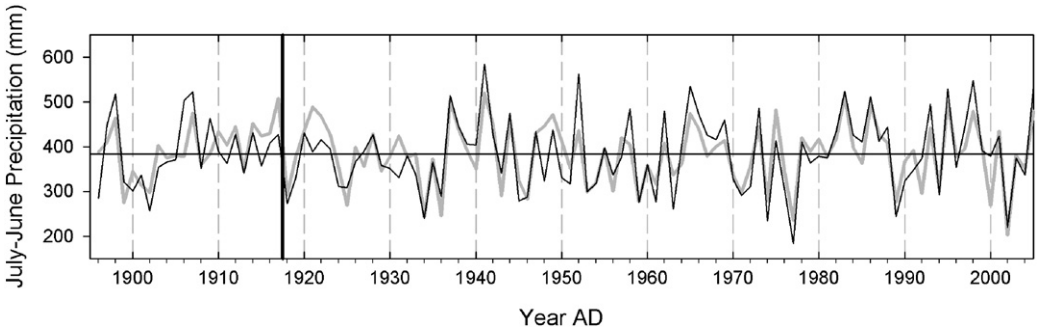

Figure 4. Time series plot showing agreement of observed and reconstructed annual July–June precipitation. Black line is PRISM observed precipitation. Gray line is tree-ring precipitation reconstructed by regression model. Vertical line marks start of calibration period (1918–2005) of model. Horizontal line is the calibration-mean observed precipitation (383 mm).

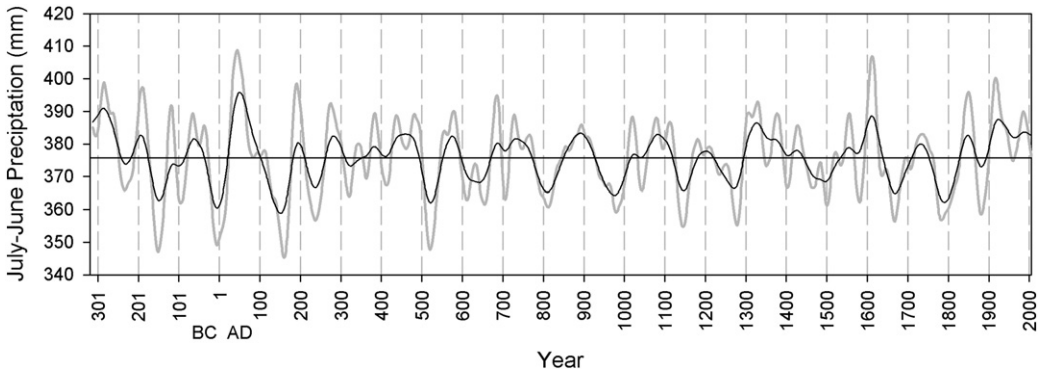

Figure 5. Smoothed long-term reconstruction showing multidecadal-to-centennial variation. Smoothing by 50-yr spline (gray) and 100-yr spline (black). Horizontal line is long-term mean reconstructed precipitation (376 mm).

during the historic period, including the extremely wet conditions of the early AD 1900s and the severe drought of the AD 1890s. We then ranked wet and dry decadal episodes by magnitude, defined as the maximum or minimum smoothed precipitation, and listed the duration and intensity of the episodes. Intensity was defined as the percentage of years exceeding the extreme dry/wet threshold in the episode.

Finally, taking advantage of the annual resolution afforded by tree rings, we identified the most extreme wet and dry years in the reconstruction. Compression of reconstructed values towards the mean, an unavoidable effect of regression, biases the direct comparison of observed and reconstructed precipitation values. Therefore, we based thresholds on reconstructed values. We identified the three wettest and driest reconstructed individual years for AD 1896–2005, the overlap of observed and reconstructed precipitation. The three driest were AD 2002 (202 mm), 1977 (236 mm) and 1934 (243 mm), and the three wettest were AD 1941 (520 mm), 1983 (513 mm), and 1917 (507 mm). Years of the long-term reconstruction were then classified as wet or dry if they were above 507 mm or below 243 mm.

Results

The precipitation reconstruction prior to AD 200 is marked by a dry phase from the early 2nd century BC to the 1st century AD and a sharp oscillation from a very wet phase to very dry phase during the first two centuries AD (Fig. 5). The magnitude of this oscillation is uncertain because the tree-ring chronology is based on only three trees during that period. However, an independently developed piñon (*Pinus edulis*) chronology from the Tavaputs Plateau shows similar oscillations (Knight, Meko, and Basain, unpublished data). After AD

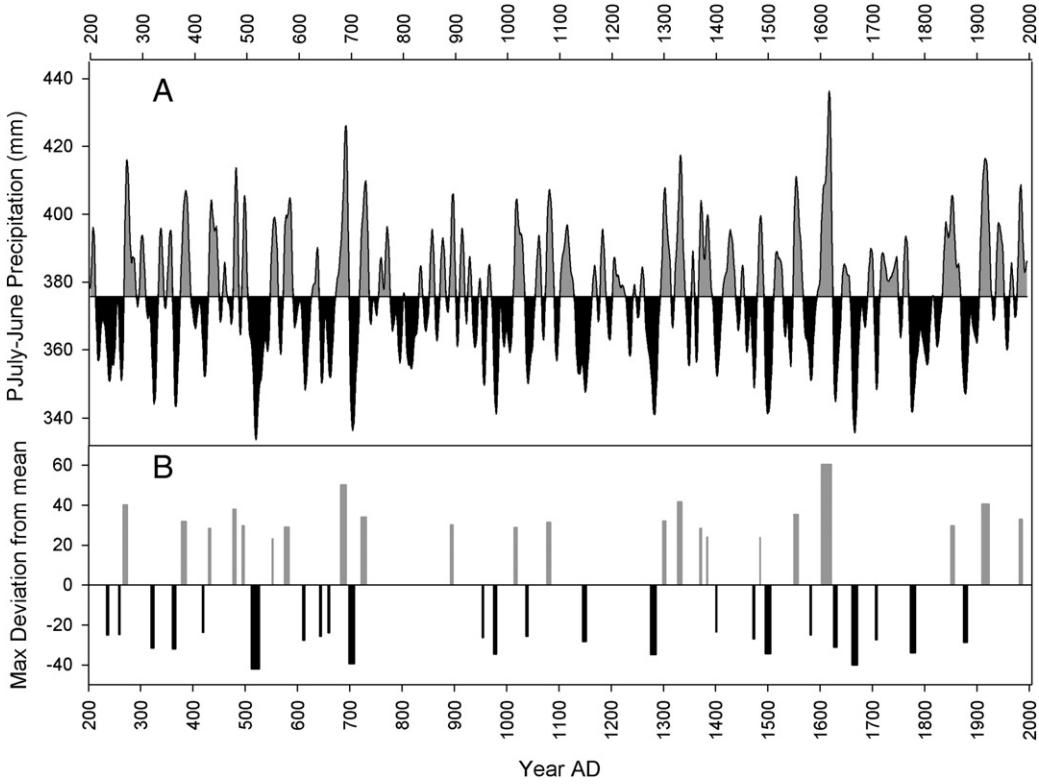

Figure 6. Time series plot showing decadal variation of reconstructed precipitation and timing of droughts and wet periods since AD 200. (A) reconstruction smoothed with 19-weight Gaussian filter. Dry episodes, or smoothed series below long-term mean, shaded black. Wet episodes, or smoothed series above mean, shaded gray. (B) Core droughts and wet periods defined as Gaussian-filtered series with standardized value exceeding 1.25 in absolute value. Height of bar represents maximum deviation of smoothed series from long term mean; width represents duration exceeding threshold.

200, long-term excursions from mean conditions occur during wet phases from AD 1300 to the early 1600s and from the mid-AD 1800s to present, and during dry phases from the early AD 1100s to 1300 and from mid-AD 1600s to mid-1800s. Between AD 500 and 1100 the series is characterized by oscillatory behavior at a wavelength of 70 to 150 yr.

Embedded within the centennial variation are numerous decadal-scale dry and wet episodes characterized by departures from the mean (Fig. 6). Statistics for episodes are listed in Table 2. Extreme magnitude, duration, and intensity of wet and dry episodes do not necessarily coincide. For instance, the dry episode AD 970–1010 lasted 41 yr but included only a 7-yr period below the "extremely dry" threshold. Conversely, the much shorter (19-yr) dry episode AD 1492–1510 included 11 yr below the threshold. Such differences emphasize the variety in time-series signatures of drought; all three properties—magnitude, duration and intensity—may be useful in gauging the strength of a dry or wet episode and its potential consequences for natural and human systems.

Two decadal episodes, one wet and one dry, stand out in terms of all three properties (Table 2). The first is the dry episode AD 502–544. This was the longest and highest magnitude dry episode, and it contained a 16-yr period below the "extremely dry" threshold. The second is the wet episode AD 1594–1623. This was the longest and highest magnitude wet episode and contained a 19-yr segment above the "extremely wet" threshold.

Abrupt transitions between the extreme categories of wet and dry occur several times in the reconstruction. For example, the transition from the wetness in the early AD 1600s (AD 1594–1623) to subsequent drought conditions is only 6 yr. Similarly, conditions switch from wet to dry, and back to wet, in a 49-yr period AD 683–731. In some cases these abrupt transitions are followed by long periods of more stable conditions. After the extreme oscillation ending in AD 731, the frequency and magnitude of extreme dry and wet periods drops and remains low until the dry period beginning in AD 1276 (Fig. 6B). This 500-yr period generally lacks decadal episodes of extreme conditions. After the wet period in the early AD 1600s, extremely wet conditions do not reemerge until the early AD 1900s—except for a brief period of wetness in the 1850s. This same interval of the early AD 1600s to early 1900s does have five extreme droughts (Fig. 6).

Table 2
Listing of ranked decadal-scale dry (A) and wet (B) periods.

Dry period—end year	(a) Max deviation from mean (cm)	(b) Length of period (yr)	(c) Mean annual deviation from mean (cm)	(d) Years below drought threshold	(e) % of period below drought threshold
(A)					
544	−42.19	43	−21.24	16	37
1688	−40.18	32	−16.13	11	34
715	−39.46	20	−33.17	11	55
1292	−34.80	30	−20.99	11	37
1010	−34.61	41	−16.16	7	17
1510	−34.45	19	−36.45	11	58
1833	−33.98	64	−15.06	10	16
372	−32.40	15	−27.72	7	47
329	−31.68	23	−18.08	6	26
1640	−31.10	17	−27.40	7	41
1904	−28.82	36	−18.72	8	22
1161	−28.30	34	−18.83	7	21
623	−27.71	35	−10.93	5	14
1713	−27.54	11	−27.65	4	36
1478	−27.02	24	−16.10	3	13
960	−26.34	29	−11.99	3	10
1052	−25.77	20	−17.68	5	25
669	−25.68	31	−21.04	3	10
263	−25.03	54	−16.98	4	7
1593	−24.93	27	−14.51	3	11
(B)					
Wet Period - end year	(a) Max deviation from mean	(b) Length of period (yr)	(c) Mean annual deviation from mean	(d) Years above pluvial threshold	(e) % of period above pluvial threshold
1623	60.51	30	34.72	19	63
695	50.35	26	28.72	11	42
1341	41.71	22	26.10	9	41
1928	40.73	24	29.11	15	63
306	40.31	43	15.96	8	19
484	38.03	11	45.21	6	55
1566	35.36	20	24.72	9	45
734	34.04	19	27.56	10	53
1996	32.97	20	15.21	6	30
1313	32.06	21	21.54	6	29
1088	31.51	16	29.77	10	63
392	31.29	20	19.03	8	40
900	30.20	13	21.89	5	38
1868	29.78	35	17.97	7	20
501	29.70	11	27.09	5	45
588	29.05	19	27.92	10	53
1032	28.76	22	19.60	6	27
446	28.41	21	26.95	5	24
1392	28.40	27	19.14	4	15
1491	23.87	13	23.50	2	15

Ranking by (a) maximum deviation of the smoothed series from long-term mean during period. Length of period (b) is number of years where smoothed series exceeds or drops below mean as in Figure 6A. Mean annual deviation from mean (c) is calculated from the unsmoothed annual reconstruction values within each period identified using the smoothed series. Years exceeding core threshold (d) is as in Figure 6B. Percentage of period exceeding core threshold (e) is 100 times ratio of (d) to (b).

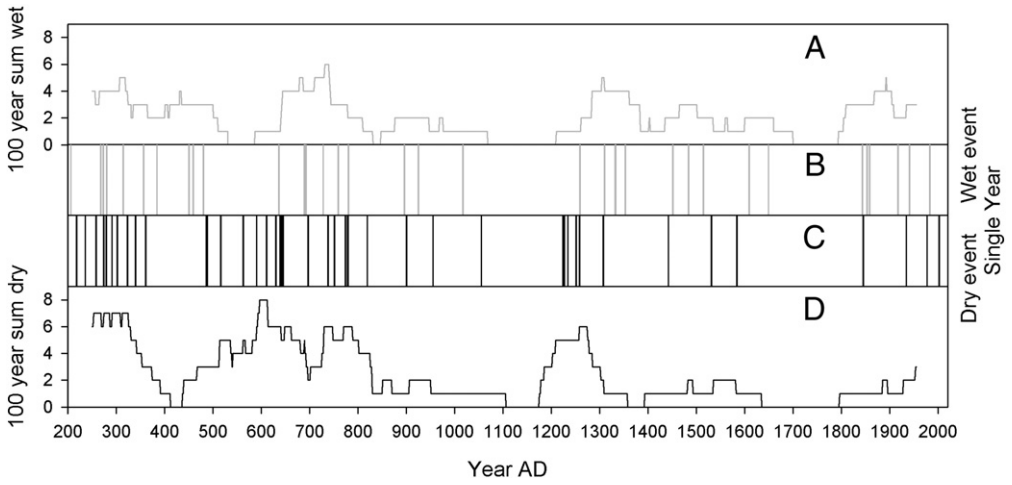

Figure 7. Extreme single-year dry and wet events. Bars indicate individual events, wet (B) and dry (C). See text for definition of events. Line graphs show sum of wet years (A) and dry years (D) in 100-yr moving window.

The identification of single-year extremes yielded 36 wet yr and 44 dry yr (Fig. 7). Extreme single-year events are unevenly distributed through time. Both wet and dry extremes cluster prior to AD 820, between AD 1220 and 1310, and again after AD 1840. Gaps or decreases in frequency of both wet and dry single-year extremes occur near AD 820–1220 and AD 1600–1840. The strong clusters prior to AD 820 are separated by shorter gaps: AD 362–485 for dry years and AD 481–635 for wet years. Consecutive years of single-year dry extremes occur only twice in the reconstruction, AD 562–563 and AD 778–779. The narrowest time-windows with three such events are 7 yr (AD 639–645) and 6 yr (AD 774–779). Extreme single-year events do not necessarily fall within or generate decadal dry and wet episodes. For instance, the wet episodes AD 1593–1623 and AD 1905–1928 are not characterized by large numbers of extreme wet years. Similarly, the severe decadal drought at the end of the AD 1200s is not characterized by a high frequency of single-year dry extremes; the dry extremes in the AD 1200s actually precede the severe decadal drought at the end of the century.

Discussion

The AD 500s drought

By several measures the AD 502–544 drought is the most severe of the Tavaputs reconstruction (Table 2). What was the larger spatial context of this drought? The question is difficult to answer because high-resolution records covering this period are rare. For a crude assessment, we assembled three of the longest and best-replicated tree-ring series, or climatic reconstructions based on them, from other parts of the American West. The series include a reconstruction of central Nevada precipitation based on the Methuselah Walk bristlecone pine (*Pinus longaeva*) chronology (Hughes and Graumlich, 1996), a reconstruction of northwestern New Mexico precipitation based on a Douglas-fir tree-ring chronology from the El Malpais lava flows (Grissino-Mayer, 1996), and a drought-sensitive western juniper chronology (*Juniperus occidentalis*) in south central Oregon (Meko et al., 2001). All three series reflect winter and spring precipitation, though the reconstruction from northwestern New Mexico probably reflects summer rainfall to some extent. All records are smoothed with a 31-yr spline to highlight decadal to multi-decadal variation.

In the Nevada and Oregon records, the early AD 500s are marked by drought, but the initiation appears slightly later than on the Tavaputs (Fig. 8). The annual reconstructed series of Tavaputs precipitation reveals the heart of the early AD 500s drought as two runs of below-average precipitation, AD 515–520 and AD 524–531. In both the Oregon and central Nevada records the AD 510s and 520s are similarly dry. In northwestern New Mexico, reconstructed precipitation is low in the AD 520s but above normal in the AD 510s. Like many other droughts of the tree-ring record, the AD 500s drought does not simultaneously hit all four of the key tree-ring sites. For instance, of the major MCA droughts—late AD 1000s, mid-1100s, and late 1200s—only the drought of the mid-AD 1100s appears at all four sites. The four series are strongly synchronous in the late AD 1500s and early 1600s, when severe drought is followed by a wet period, and in the late AD 100s during a high-magnitude wet period (Fig. 8).

To further refine our view of the extent of the AD 500s drought we looked at several other records available for the period. In two other moisture-sensitive millennial length tree-ring chronologies (not shown) recently developed in eastern and southeastern Utah, the early AD 500s appear as prominent low-growth feature (Knight, Meko, and Basain, unpublished data). Remnant-wood Douglas-fir samples from Eagle, Colorado, near the headwaters of the Colorado River, also show the early AD 500s as a low-growth interval (data provided by Connie Woodhouse).

Farther west, in the Sierra Nevada, evidence for extreme drought in the first half of the AD 500s is lacking. Giant Sequoia (*Sequoiadendron giganteum*) chronologies that cover this interval do no show a marked increase in frequency of very narrow rings (Hughes and Brown, 1992), while fire frequency in giant sequoia groves actually decreases (Swetnam, 1993). Hughes and Brown (1992) note, however, that giant sequoia tree rings are much better recorders of extremely dry single years than of multi-year extended dry periods. The sequoia record cannot therefore be regarded as strong evidence for absence of an early AD 500s drought in the Sierra Nevada.

In summary, a synthesis of information from long chronologies suggests the severe early AD 500s drought on the Tavaputs was part of a larger feature affecting at least parts of the Upper Colorado River Basin (UCRB), Great Basin and Pacific Northwest. This pattern is consistent with a contraction of the westerlies and withdrawal of the winter storm track to the north over western North America. Normal or high growth at tree-ring sites further to the south (e.g., New Mexico, Arizona) could still occur under these conditions with enhanced summer monsoon rainfall, or possibly with low-latitude storms undercutting a ridge over the western United States.

Medieval climate anomaly on the Tavaputs

The Tavaputs reconstruction gives an 1800-yr perspective on the moisture conditions between AD 800 and AD 1300 for a particular

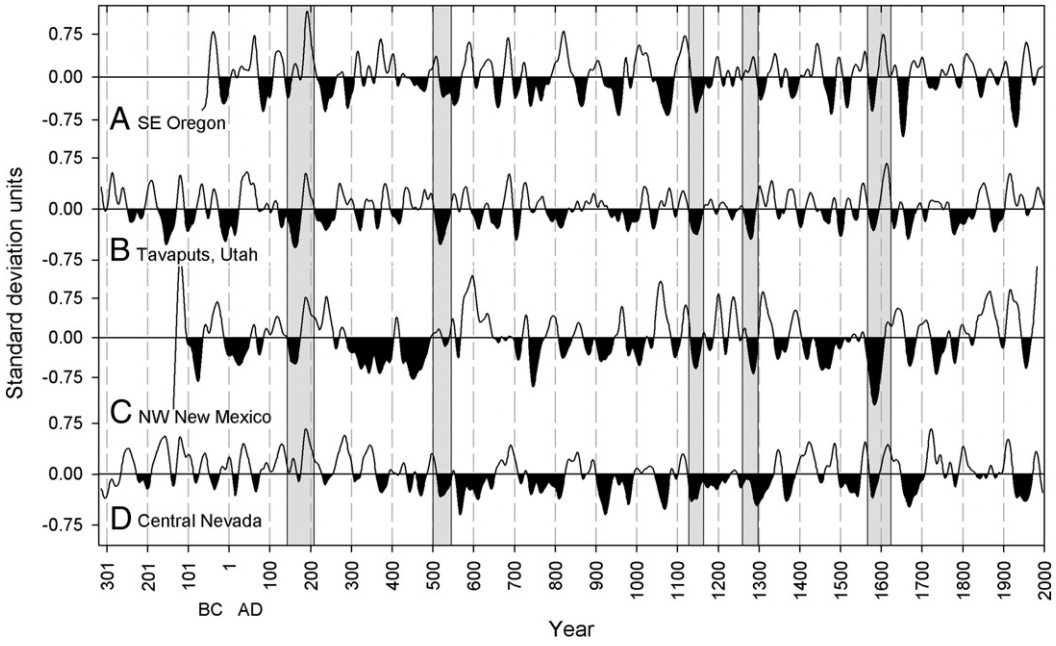

Figure 8. Comparison of Tavaputs precipitation reconstruction with other regional tree-ring climate reconstructions and a long moisture sensitive tree-ring chronology. Periods mentioned in text are shaded gray for emphasis. (A) Table Rock, Oregon, western juniper (*Juniperus occidentalis*) tree-ring chronology (Meko et al., 2001), (B) Tavaputs July–June precipitation reconstruction, (C) northwestern New Mexico climate-division 4 July–June precipitation reconstruction from El Malpais tree-ring chronology (Grissino-Mayer, 1996), (D) central Nevada climate-division 3 July–June precipitation reconstruction, from Methuselah Walk bristlecone pine chronology (Hughes and Graumlich, 1996), All series were converted to standard deviation units and smoothed with a 31-yr spline. See map in Figure 1 for locations of series.

location. From the AD 1130s to 1300 the Tavaputs is indeed dry, contrasting sharply with the wetness after AD 1300 (Fig. 5). Prolonged dry conditions also occur prior to AD 830 and again in the mid-to-late AD 900s, while wetter conditions are especially pronounced in the AD 1000s. High-amplitude low-frequency fluctuation rather than overall dryness characterizes the broader MCA interval. Other centennial-length dry periods, such as the mid-1600s to mid-1800s, rival those of the AD 1100s and 1200s. With decadal-scale smoothing (Fig. 6) droughts in the late AD 900s, mid-1100s and late 1200s are persistent, but their duration and magnitude are not unique (Table 2). Are the prolonged MCA droughts unusually clustered? Of the 20 highest-magnitude dry episodes (Table 2) five occur between AD 800 and 1300; these have an average duration of 33 yr. Five dry periods also occur in the previous 500-yr period, AD 300–800, while six and part of a seventh occur in the subsequent 500-yr period, AD 1300–1800. The average duration of dry periods is 28 yr both for AD 300–800 and AD 1300–1800. While high-magnitude droughts in the MCA are not unusually frequent, they are somewhat atypically long.

Other properties of the MCA as reconstructed on the Tavaputs merit attention. At the decadal scale, the record shows both rapid oscillations such as during the AD 800s and early AD 900s, and broader swings such as during the late AD 900s to mid-1100s. Both single-year (Fig. 7) and decadal-scale (Fig. 6) wet and dry extremes decrease in frequency and magnitude between AD 800 and 1200. Variance of reconstructed precipitation in moving 20- and 100-yr windows reaches its all-time low between AD 950 and 1200, the core of the MCA. Although our reconstruction marks the MCA as unusual in a few aspects of drought variability, the period stands out in the archaeological record of the Tavaputs Plateau. Between AD 1000 and 1300, people who lived a semi-sedentary lifestyle and practiced agriculture flourished in the canyons of the plateau (Spangler, 2000). Several features presented here, such as sustained droughts in the AD 1100s and 1200s and a lack of extremes prior to AD 1200, may have important archaeological implications for the eventual abandonment of agriculture by AD 1300 (Benson et al., 2007; Kloor, 2007).

20th century in long-term perspective

Is the instrumental record reflective of the range of natural climate variability for northeastern Utah? In short, we find the answer mixed. Prolonged and at times extremely intense droughts are a regular part of the Tavaputs long reconstruction but are absent from the modern record. This conclusion is consistent with two recent tree-ring-based moisture reconstructions for northeastern Utah (Gray et al., 2004; MacDonald and Tingstad, 2007). Our reconstruction classifies the modern period as wet in the context of the last 1800 yr, but not as wet as the early AD 1600s or possibly the early AD 1300s. The anomalous wetness of the 20th century has been pointed out in several paleoclimatic reconstructions for the West (Stine, 1994; Grissino-Mayer, 1996; Woodhouse et al., 2006; Stahle et al., 2007).

The implications for water management in the West are significant. Growing populations fueling increased demand have already placed stress on available resources. The current (1999–2008) drought, which sent Lake Powell on the Colorado River to record low levels (U.S. Bureau of Reclamation www.usbr.gov/uc/feature/drought.html), has been relatively brief in the context of the past two millennia. Yet this recent drought has raised the specter of severe water shortages with projected increasing temperatures (McCabe and Wolock, 2007).

The instrumental period does provide examples of what may be the most extreme short-term drought conditions. AD 2002 (6th driest), 1977 (34th driest) and 1934 (45th driest) are among the driest 3% of individual years in the reconstruction since AD 200. The worst-case scenario for water management may be the occurrence of one or more of these extreme years embedded in an extended dry period. An example from the past is the dry AD 600s, when four extremely dry years occur in the 15-yr interval AD 630–645. Such conditions could be stressful even for water-supply systems with considerable multi-year storage.

The extreme drought year AD 2002 emphasizes the potential impact on ecological systems of short-duration extreme events embedded within longer-duration droughts. AD 2002 witnessed both regional and local die-off of pinyon (*Pinus edulis*), a widespread

and ecologically important woodland dominant. The die-off most likely resulted from both direct drought mortality and weakened resistance to lethal bark beetles and other pests (Breshears et al., 2005). This die-off, though primarily driven by short-term extreme conditions, will have consequences that persist on the landscape for decades (Allen and Breshears, 1998). Return to a more persistent drought regime like those seen in past centuries could heighten the effects of such extreme years on water resources and ecosystems.

Drivers of climatic variability on the Tavaputs

Recent studies have linked UCRB precipitation and streamflow variability with remote atmospheric and oceanic oscillations, including the El Niño Southern Oscillation (ENSO), the Pacific Decadal Oscillation (PDO) and the Atlantic Multi-decadal Oscillation (AMO) (Hidalgo and Dracup, 2003; McCabe et al., 2007). On the inter-annual time scale, ENSO is a major contributor to climatic variability in the west. During El Niño episodes (warmer eastern tropical Pacific) the Pacific Northwest tends to be drier than normal and the southwestern US wetter than normal, and vice-versa during La Niña episodes (cooler eastern tropical Pacific) (Brown and Comrie, 2004). The UCRB lies in a transition zone between these poles. Much of Utah and southern Colorado responds as the southwestern US; the upper Green River Basin weakly responds as the Pacific Northwest; and the headwaters area in Colorado shows little correspondence with either pole (Hidalgo and Dracup, 2003; Woodhouse, 2003; Woodhouse et al., 2006). As mapped by Hidalgo and Dracup (2003), the Tavaputs falls clearly within the part of the UCRB whose ENSO response is like that of the southwestern US. We confirmed this through correlation of monthly and seasonal composites of the Tavaputs PRISM derived precipitation data with June-November Southern Oscillation Index (SOI), a measure of ENSO state, downloaded from NOAA's Climate Prediction Center (http://www.cpc.ncep.noaa.gov/data/indices/). Tavaputs precipitation is negatively correlated with SOI (June–July precipitation, 1933–2005, $r=-0.47$, $\alpha=0.01$), indicating wetter (drier) conditions during El Niño (La Niña). Examination of specific El Niño/La Niña events suggests this relationship is dominated by wetter conditions during El Niño, and that dry years are unrelated to La Niña events.

At the decadal to multi-decadal scale, shifts in the PDO and AMO may influence UCRB moisture variability, perhaps changing the spatial pattern of ENSO relationships within the UCRB by shifting the ENSO dipole transition zone (Hidalgo and Dracup, 2003). Anomalies in Tavaputs reconstructed precipitation indeed sometimes track inferred or reconstructed moisture conditions in Oregon (e.g., AD 680s–730s) and other times in New Mexico (e.g., AD 1260s–1340s) (Fig. 8). In general, warm North Atlantic sea-surface temperatures appear to be associated with 20th century UCRB drought (McCabe et al., 2007), while PDO tends to enhance ENSO teleconnections, strengthening El Niño effects during its positive (colder north Pacific) phase, and La Niña effects during its negative (warmer north Pacific) phase (Gershunov and Barnett, 1998; Timilsena et al., 2009). That Tavaputs precipitation is weakly positively correlated with the PDO ($r=0.272$, $\alpha=0.01$) is consistent with enhancement of El Niño effects by colder north Pacific sea-surface temperatures. The two driest decades of the instrumental record, however, AD 1970–1979 and 1926–1935, occurred during opposite PDO phases, suggesting this relationship is complicated by other factors.

Gridded tree-ring reconstructions of moisture conditions for North America have given insights into spatial patterns of drought and their possible forcing factors over the past 1200 yr (Cook et al., 2004; Herweijer et al., 2007; Stahle et al., 2007). The reconstructions can be linked to remote forcing factors either by analogy with modern droughts or by independent reconstruction of the forcing factors themselves (Graham et al., 2007; Seager et al., 2007). For example, MCA droughts in the 10th, 12th, and 13th centuries have been linked to winter-precipitation decreases possibly associated with persistent La Niña-like conditions driven by greater solar forcing and/or a lack of volcanic activity (Graham et al., 2007; Seager et al., 2007).

For earlier droughts, mapping of spatial patterns of drought and attribution of possible forcing factors becomes more and more difficult as the number proxy records diminishes with time. The early AD 500s drought is a case in point. The four records plotted in Fig. 8 suggest the AD 500s drought had a northwest dry/southwest wet pattern, which is consistent with El Niño. That the Tavaputs is one of the dry sites suggests the El Niño transition zone was shifted to the south.

For a broader spatial footprint of drought during years with New Mexico being wet and the other three locations dry (below −0.5 standard units), we examined gridded PDSI maps of Cook et al. (2008). For the common period of the four series (66 BC to AD 1992) such conditions occurred in a total of 28 yr, including 3 yr during the early AD 500s drought. The analysis of PDSI maps was restricted to the period after AD 800, when the number of tree-ring chronologies contributing to the PDSI reconstructions increases sharply. Fourteen of the 28 selected spatial-contrast years occurred after AD 800. The PDSI maps for those years were consistent with the moisture anomalies at the four key locations in showing Oregon dry and New Mexico wet. Three distinct larger scale patterns of drought were represented in the 14 maps: (1) drought centered on the interior northwest and extending south into central California and east into the northern and central Rockies, (2) drought similar to the first pattern but shifted southwards, with normal to wet conditions in western Canada and Washington, and (3) dry across nearly the entire continent, with strongest drought in a band across the northern and central Rockies and Plains, and less dry to neutral moisture conditions in southern California and the Southwest. The first two patterns are an El Niño/La Niña signature with the transition zone shifted south (case 1) or north (case 2). The third pattern recalls the 1930s "Dust Bowl" drought, associated with a warm North Atlantic, cool eastern tropical Pacific and a lack of El Niño events (Cook et al., 2007). Analysis of the PDSI maps by Cook et al. (2007) revealed this pattern to be relatively rare over the last 1000 yr. Thus, the early AD 500s drought could be a significant earlier example of this pattern.

Conclusions

The Tavaputs reconstruction provides several insights on local and regional climate history. The frequency and magnitude of wet and dry extremes, both annual and decadal, has changed through time, and only some past droughts and wet periods have analogues in the modern era. The diverse time-series signatures of droughts and wet periods in the tree-ring record emphasize the need to study climate series at multiple temporal scales. The reconstruction presented here helps quantify the natural range of variability, evaluate whether the instrumental record adequately reflects this variability, and identifies periods of time and events potentially significant to ecosystem and human history.

One such period with no analogue is the early AD 500s. A drought in the early AD 500s was identified as the most severe drought in the last 1800 yr of the reconstruction. The runs of dry years experienced then could have severe impacts on a society not prepared to deal with them. The small set of available tree-ring records of moisture conditions in the AD 500s suggests spatial patterns of moisture anomaly like those in El Niño/La Niña events and the 1930s "Dust Bowl". The data also hint at decadal to multi-decadal shifts in the transition zone of the El Niño/La Niña dipole. Increased density of tree-ring coverage during the first millennium AD will be essential for refining these preliminary conclusions. Our reconstruction supports other proxy records in suggesting that the period AD 800–1300 was characterized by a series of prolonged and

severe droughts. On the Tavaputs Plateau, however, these droughts were not unique in length or magnitude. This period does stand out for decreased variance and extremes, both decadal and annual. These characteristics may have important implications for understanding the regional archaeology.

Remnant-wood collections at lower elevations in the West have the potential to greatly extend our knowledge of the climate history of the region and thereby gain further understanding of the range of natural variability and change. Potential applications include identifying analogues for future climate change, examining the effects of climate on ecosystems and human populations, and ultimately assessing the causes and drivers of climate in the region. From collections made in 2005 we discovered three locations in eastern Utah that harbored remnant wood with rings prior to AD 500. In this paper we presented a precipitation reconstruction from the longest and best-replicated of these collections. Despite the already dense network of climatically sensitive tree-ring sites in the western United States, there remains significant potential for extending dendroclimatic reconstructions by focusing future efforts on remnant-wood collection.

Acknowledgments

This work was financially supported by grants from the Explorers Club Exploration Fund, the National Science Foundation IGERT Program in Archaeological Science at the University of Arizona, and the U.S. Bureau of Reclamation (award 04-FG-32-0260). We thank Erica Bigio and Erika Wise for their assistance in the field, and Erin Brannon for her assistance in the lab. We also thank Jeffrey Dean, Connie Woodhouse, and two anonymous reviewers for their valuable comments and suggestions on earlier drafts of this paper.

References

Allen, C.D., Breshears, D.D., 1998. Drought-induced shift of a forest-woodland ecotone: rapid landscape response to a climate variation. Proceedings of the National Academy of Sciences 95, 14839–14842.

Bloomfield, P., 2000. Fourier Analysis of Time Series: An Introduction, second edition. John Wiley & Sons, Inc., New York, p. 261.

Breshears, D.D., Cobb, N.S., Rich, P.M., Price, K.P., Allen, C.D., Balice, R.G., Romme, W.H., Kastens, J.H., Floyd, M.L., Belnap, J., Anderson, J.J., Myers, O.B., Meyer, C.W., 2005. Regional vegetational die-off in response to global-change-type drought. Proceedings of the National Academy of Science 102 (42), 15144–15148.

Benson, L., Kashgarian, M., Rye, R., Lund, S., Paillet, F., Smoot, J., Kester, C., Mensing, S., Meko, D., Lindström, S., 2002. Holocene multidecadal and multicentennial droughts affecting Northern California and Nevada. Quaternary Science Reviews 21, 659–682.

Benson, L.V., Berry, M.S., Jolie, E.A., Spangler, J.D., Stahle, D.W., Hattori, E.M., 2007. Possible impacts of early 11th, middle 12th, and late 13th century droughts on western Native Americans and the Mississippian Cahokians. Quaternary Science Reviews 26, 336–350.

Brown, D.P., Comrie, A.C., 2004. A winter 'dipole' in the western United States associated with multidecadal ENSO variability. Geophysical Research Letters 31, L09203.

Carson, E.C., Munroe, J.S., 2005. Tree-ring based streamflow reconstruction for Ashley Creek, northeastern Utah: implications for palaeohydrology of the southern Uinta Mountains. The Holocene 15 (4), 602–611.

Cook, E.R., 1985. *A Time Series Approach to Tree-Ring Standardization*. Ph.D. dissertation, University of Arizona, Tucson.

Cook, E.R., Peters, K., 1981. The smoothing spline: a new approach to standardizing forest interior tree-ring width series for dendroclimatic studies. Tree-Ring Bulletin 41, 45–53.

Cook, E.R., Briffa, K.R., Meko, D.M., Graybill, D.S., Funkhouser, G., 1995. The 'segment length curse' in long tree-ring chronology development for paleoclimatic studies. The Holocene 5 (2), 229–237.

Cook, E.R., Woodhouse, C.A., Eakin, C.M., Meko, D.M., Stahle, D.W., 2004. Long-term aridity changes in the western United States. Science 306, 1015–1018.

Cook, E.R., Seager, R., Cane, M.A., Stahle, D.W., 2007. North American drought: reconstructions, causes, and consequences. Earth-Science Reviews 81, 91–134.

Cook, E.R., et al., 2008. North American Summer PDSI Reconstructions, Version 2a. IGBP PAGES/World Data Center for Paleoclimatology. Data Contribution Series # 2008-046. NOAA/NGDC Paleoclimatology Program, Boulder CO, USA.

Davies, R.B., Harte, D.S., 1987. Tests for the Hurst effect. Biometrika 74, 95–102.

Dean, J.S., Euler, R.C., Gumerman, G.G., Plog, F., Hevly, R.H., Karlstrom, T.N.V., 1985. Human behavior, demography, and the paleoenvironment on the Colorado Plateaus. American Antiquity 50 (3), 537–554.

Deitrich, C.R., Newsam, G.N., 1997. Fast and exact simulation of stationary Gaussian processes through circulant embedding of the covariance matrix. SIAM Journal on Scientific Computing 18 (4), 1088–1107.

Fritts, H.C., 1976. Tree Rings and Climate. The Blackburn Press, Caldwell, New Jersey.

Fritts, H.C., Guiot, J., Gordon, G.A., 1990. Verification. In: Cook, E.R., Kairiukstis, L.A. (Eds.), Methods of Dendrochronology, Applications in the Environmental Sciences. Kluwer Academic Publishers, pp. 178–185.

Graham, N.E., Hughes, M.K., Ammann, C.M., Cobb, K.C., Hoerling, M.P., Kennett, D.J., Kennett, J.P., Rein, B., Stott, L., Wigand, P.E., Xu, T., 2007. Tropical Pacific – mid latitude teleconnections in medieval times. Climatic Change 83, 241–285.

Gray, S.T., Jackson, S.T., Betancourt, J.L., 2004. Tree-ring based reconstructions of interannual to decadal precipitation variability for northeastern Utah since 1226 A.D. Journal of the American Water Resources Association 40, 940–960.

Grissino-Mayer, H.D., 1996. A 2129-year reconstruction of precipitation for northwestern New Mexico. In: Dean, J.S., Meko, D.M., Swetnam, T.W. (Eds.), Tree-rings, Environment, and Humanity. Radiocarbon, Tucson, pp. 191–204.

Gershunov, A. and Barnett, T.P., 1998. Interdecadal modulation of ENSO teleconnections. Bulletin of the American Meteorological Society.

Herweijer, C., Seager, R., Cook, E.R., Emile-Geay, J., 2007. North American droughts of the last millennium from a gridded network of tree-ring data. Journal of Climate 20, 1353–1376.

Hidalgo, H.G., Dracup, J.A., 2003. ENSO and PDO effects of hydroclimatic variations of the upper Colorado River Basin. Journal of Hydrometeorology 4, 5–23.

Holmes, R.L., 1983. Computer assisted quality control in tree-ring dating and measurement. Tree-Ring Bulletin 43, 69–78.

Hughes, M.K., Brown, P.M., 1992. Drought frequency in central California since 101 B.C. recorded from giant sequoia tree rings. Climate Dynamics 6, 161–167.

Hughes, M.K., Diaz, H.F., 1994. Was there a "Medieval Warm Period", and if so, where and when? Climatic Change 26, 109–142.

Hughes, M.K., Funkhouser, G., 1998. Extremes of moisture reconstructed from tree-rings. In: Beniston, M., Innes, J.L. (Eds.), The Impacts of Climate Variability on Forests. Lecture Notes in the Earth Sciences, 74. Springer-Verlag, Berlin, pp. 99–107.

Hughes, M.K., Graumlich, L.J., 1996. Multimillennial dendroclimatic records from western North America. In: Bradley, R.S., Jones, P.D., Jouzel, J. (Eds.), Climatic Variations and Forcing Mechanisms of the Last 2000 Years. Springer Verlag, Berlin, pp. 109–124.

Kloor, K., 2007. The Vanishing Fremont. Science 318, 1540–1543.

MacDonald, G.M., Tingstad, A.H., 2007. Recent and multicentennial precipitation variability and drought occurrence in the Uinta Mountains region, Utah. Arctic, Antarctic and Alpine Research 39 (4), 549–555.

McCabe, G.J., Wolock, D.M., 2007. Warming may create substantial water supply shortages in the Colorado River basin. Geophysical Research Letters 34, L22708.

McCabe, G.J., Betancourt, J.L., Hidalgo, H.G., 2007. Associations of decadal to multidecadal sea-surface temperature variability with upper Colorado River flow. Journal of the American Water Resources Association 43 (1), 184–192.

Meko, D.M., Woodhouse, C.A., 2005. Tree-ring footprint of joint hydrologic drought in Sacramento and Upper Colorado river basins, western USA. Journal of Hydrology 308, 196–213.

Meko, D.M., Therrell, M.D., Baisan, C.H., Hughes, M.K., 2001. Sacramento River flow reconstructed to A.D. 869 from tree rings. Journal of the American Water Resources Association 37 (4), 1029–1040.

Meko, D.M., Woodhouse, C.A., Baisan, C.A., Knight, T., Lukas, J.L., Hughes, M.K., Salzer, M.W., 2007. Medieval drought in the upper Colorado River Basin. Geophysical Research Letters 34, L10705.

Michaelsen, J., 1987. Cross-validation in statistical climate forecast models. Journal of Climate and Applied Meteorology 26, 1589–1600.

Mitchell, V.L., 1976. The regionalization of climate in the Western United States. Journal of Applied Meteorology 15, 920–927.

Mock, C.J., 1996. Climatic controls and spatial variations of precipitation in the western United States. Journal of Climate 9, 1111–1125.

Percival, D.B., Constantine, W.L.B., 2006. Exact simulation of Gaussian time series from nonparametric spectral estimates with application to bootstrapping. Statistics and Computing 16 (1), 25–35.

Peterson, K.L., 1994. A warm and wet little climatic optimum and a cold and dry Little Ice Age in the southern Rocky Mountains, U.S.A. Climatic Change 26, 243–269.

Seager, R., Graham, N., Herweijer, C., Gordon, A.L., Kushnir, Y., Cook, E., 2007. Blueprints for Medieval hydroclimate. Quaternary Science Reviews 26, 2322–2336.

Snee, R.D., 1977. Validation of regression models: methods and examples. Technometrics 19, 415–428.

Spangler, J.D., 2000. Radiocarbon dates, acquired wisdom, and the search for temporal order in the Uinta Basin. In: Madsen, D.B., Metcalf, M.D. (Eds.), Intermountain Archaeology. University of Utah Anthropological Papers No. 122. University of Utah Press, Salt Lake City, UT, pp. 48–99.

Stahle, D.W., Fye, F.K., Cook, E.R., Griffin, R.D., 2007. Tree-ring reconstructed megadroughts over North America since A.D. 1300. Climatic Change 83, 133–149.

Stine, S., 1994. Extreme and persistent drought in California and Patagonia during medieval time. Nature 269, 546–549.

Stokes, M.A., Smiley, T.L., 1968. An Introduction to Tree-Ring Dating. University of Arizona Press, Tucson.

Swetnam, T.W., 1993. Fire history and climate change in giant sequoia groves. Science 262, 885–889.

Taylor, G.H., Daly, C., and Gibson, W.P., 1995. Development of a model for use in estimating the spatial distribution of precipitation. *Proceedings of the 9th Conference on Applied Climatology, Dallas TX*, American Meteorological Society pp.92–93.

Timilsena, J., Piechota, T., Tootle, G., Singh, A., 2009. Associations of interdecadal/interannual climate variability and long-term Colorado River Basin streamflow. Journal of Hydrology 365, 289–301.

Wigley, T.M.L., Briffa, K.R., Jones, P.D., 1984. On the average value of correlated time series, with applications in dendroclimatology and hydrometeorology. Journal of Climate and Applied Meteorology 23, 201–213.

Woodhouse, C.A., 2003. A 431-yr reconstruction of western Colorado snowpack from tree-rings. Journal of Climate 16, 1551–1561.

Woodhouse, C.A., Gray, S.T., Meko, D.M., 2006. Updated streamflow reconstructions for the Upper Colorado River Basin. Water Resources Research 42, W05415.